

Microstructural and magnetic behavior of an equiatomic NiCoAlFe alloy prepared by mechanical alloying

C.D. Gómez-Esparza, F.J. Baldenebro-López, C.R. Santillán-Rodríguez, I. Estrada-Guel, J.A. Matutes-Aquino, **J.M. Herrera-Ramírez**, R. Martínez-Sánchez

Abstract

Equiatomic NiCoAlFe powder alloys were synthesized by mechanical alloying. The microstructural evolution of the mechanically alloyed powders at different times was followed with X-ray diffraction and scanning electron microscopy. The as-mechanically alloyed powders were subjected to a rapid annealing treatment at 1273 K and 1473 K during 3 min in vacuum. X-ray diffraction studies show the structure of both, the as-mechanically alloyed and annealed powders, consisted in a mixture of nanocrystalline simple phases (FCC + BCC). Crystallite size, after annealing, still remained in nanoscale. Coercivity increased due to the decrease in crystallite size and because of the defects caused by mechanical alloying in the as-mechanically alloyed samples; then coercivity decreased due to the phenomenon of random magnetic anisotropy and tended to stabilize with longer alloying times. A similar behavior was observed in annealed samples at 1273 K. However, random magnetic anisotropy was not observed after annealing at 1473 K because crystals with larger sizes were produced, and a steady increase in coercivity was observed.

1. Introduction

The design of traditional alloys is limited to the use of one or two elements as major constituents, with a maximum of four elements, and small additions of other elements to improve their properties. Based on the effect of mixing entropy, Yeh et al. [1] established that alloys could be divided into three groups: low-entropy alloys,

which are the traditional alloys; high-entropy alloys are those which consist of at least five principal elements; and medium-entropy alloys containing from 2 to 4 major alloying elements. The effect of high entropy is the preference of the systems for the formation of disordered solid solutions, which is primarily found in the alloys of high entropy and less common in the medium-entropy alloys. It is known that the alloying elements directly affect the microstructure and properties of these alloys [2]. Additionally, nanostructured materials often exhibit very different properties from their respective bulk materials. In this regard, the synthesis route is an important factor that affects the micro-structure and final properties of products, additional to the alloying elements effect. Nanostructured materials can be synthesized by several routes, being the mechanical alloying (MA) process one of them [3].

The MA technique is a solid state route which can produce a variety of phases in equilibrium and non-equilibrium state. It is possible to synthesize alloys or solid solutions from pure element powder having nanocrystalline structures and unusual properties with the MA technique. One advantage of this technique is that its process parameters can be easily modified and controlled [3].

Nanocrystalline alloys have great potential in technological applications. Alloys with transition elements like Fe, Co and Ni, are magnetic materials whose properties such as coercivity, magnetization and magnetic anisotropy are of interest, as well as the study of their microstructure that directly affects their magnetic properties [4,5].

From a scientific point of view, it is relevant a study of the influence of milling time and heat treatments on microstructural and magnetic behavior of a

nanocrystalline equiatomic NiCoAlFe alloy produced by MA.

2. Experimental

Equiatomic NiCoAlFe alloys were prepared by high-energy ball milling, using elemental powders of Ni, Co, Al and Fe, with particle size of -300, -325, -325 and -200 meshes, and purity of 99.8%, 99.5%, 99.5% and 99.0%, respectively. The alloying process was performed with 0, 10, 20 and 30 h in a SPEX-8000 M high-energy mill.

Table 1
Variation of chemical compositions as a function of alloying time (at.%).

Alloying time (h)	Ni	Co	Al	Fe
0	25 ^a	25 ^a	25 ^a	25 ^a
10	25	28	22	25
20	25	28	22	25
30	23	28	23	26

^a Nominal composition.

Cycles of 1 h alloying and 0.5 h resting were performed in order to avoid overheating of samples. The powders were sealed under an argon atmosphere to avoid components oxidation in a hardened steel vial. A milling media/sample ratio of 5/1 (in weight) was kept for all experimental runs. Methanol was used as a process control agent (PCA) to avoid the agglomeration of metal particles. The as-mechanically alloyed powders were then annealed at two different temperatures (1273 and 1473 K) for 3 min in sealed quartz ampoule in vacuum, using a Carbolite STF horizontal tube furnace.

The particle size distribution of as-mechanically alloyed powders was measured using laser diffraction and scattering with a Mastersizer-2000 particle size

analyzer. The morphological evolution of the powders was observed by scanning electron microscopy (SEM) in a JEOL JSM-5800LV microscope supplied with an energy dispersive spectrometer (EDS), while the microstructural features of individual metal particles were determined with a field-emission scanning electron microscope JEOL JSM-7401F. Transmission electron microscopy (TEM) analyses were done utilizing an aberration-corrected JEOL-JEM2200FS transmission electron microscope. The X-ray diffraction (XRD) tests were performed in a Panalytical X'Pert PRO diffractometer with Cu Ka radiation ($\lambda = 0.15406$ nm), using 35 kV and 25 mA. The step and acquisition time were 0.1° and 100 s, respectively. The HighScore software that supports measurements of PANalytical XRD instruments was used to determine the crystallite size of the mechanically alloyed (MA'ed) samples, through measurement of the half-peak width.

Magnetic properties were measured at 300 K in a physical property measurement system (PPMS), under a maximum applied magnetic field of 40 kOe.

3. Results and discussion

Table 1 shows the chemical composition of as-mechanically alloyed samples based on results of the EDS–SEM analyses. Although this technique is limited to being semi-quantitative, it was used to confirm that the chemical composition of the alloys were nearly equiatomic.

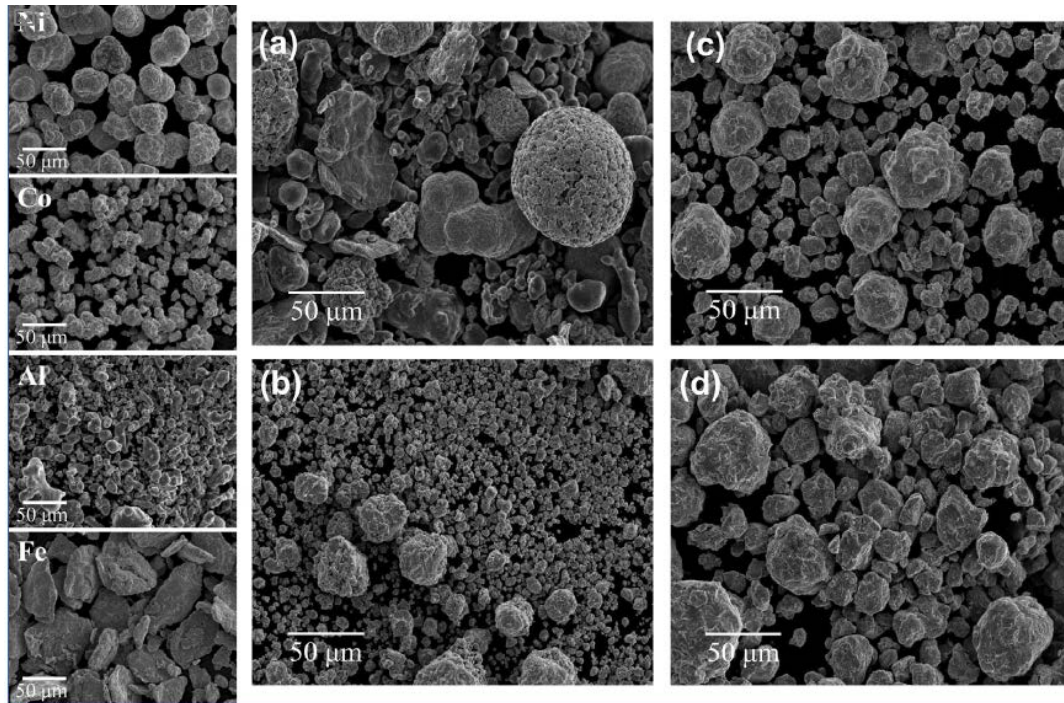


Fig. 1. SEM micrographs of MA'ed NiCoAlFe powder alloy. (a) The starting powders mixture and alloyed for: (b) 10 h, (c) 20 h and (d) 30 h. The starting elemental powders (Ni, Co, Al and Fe) are shown in the left part of the figure.

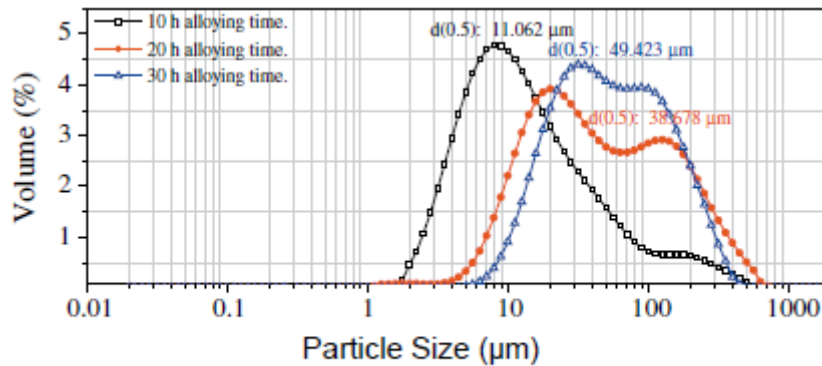


Fig. 2. Particle size distribution curves of NiCoAlFe alloy.

It is possible to assume a good chemical homogeneity of the powder alloys with a variation of $\pm 3\%$ even on those ones obtained during lower alloying times.

Milling process has an important effect over the morphology of milled products. The intrinsic mechanical characteristics of powder as well as their volumetric fractions affect the surface characteristics. Raw materials and as-alloyed

powders were analyzed by SEM. Some representative micrographs are presented in Fig. 1. The as-received pure elemental powders exhibit different morphologies: nickel, angular; cobalt, irregular; aluminum, rounded and iron, flake shape.

The particles are cold welded forming larger particles at early stages of milling process. The agglomerated particles are exposed to a continuous process of fracture and cold welding with further milling. This facilitates the atomic diffusion process and then the alloying process takes place. In Fig. 1a, a mixture of powder particles of different materials is evident. After alloying process (Fig. 1b–d), a homogeneous morphology can be achieved with the continuous competition between plastic deformation, agglomeration and size reduction. At the same time, the chemical composition of individual MA'ed powder is very similar to the proportion of the starting elemental powders, which was corroborated based on EDS–SEM analyses (Table 1).

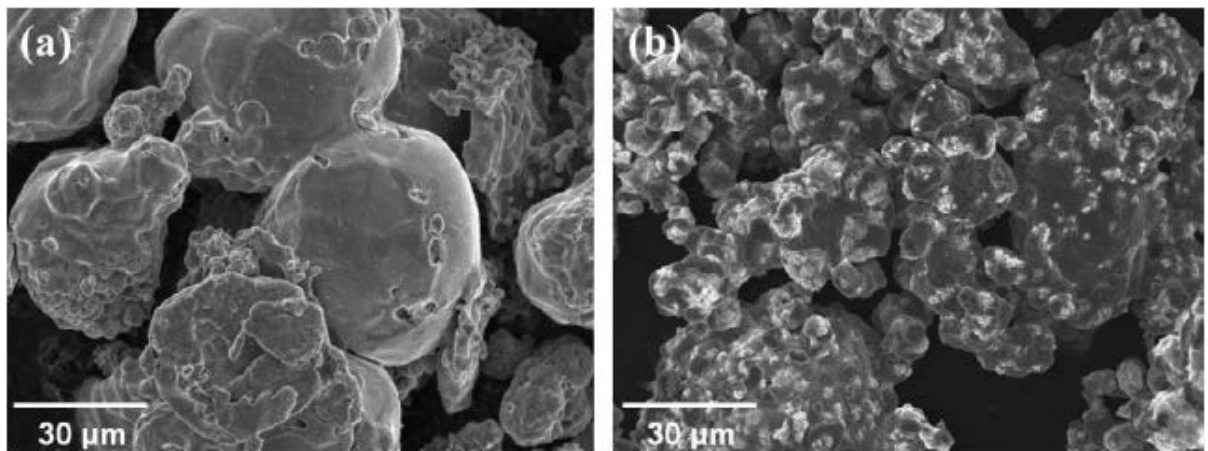


Fig. 3. SEM images of equiatomic NiCoAlFe alloys: (a) mixture of elemental powders after annealing at 1273 K, (b) mechanically alloyed powders for 10 h and annealed at 1473 K. An incipient sintering between particles can be observed.

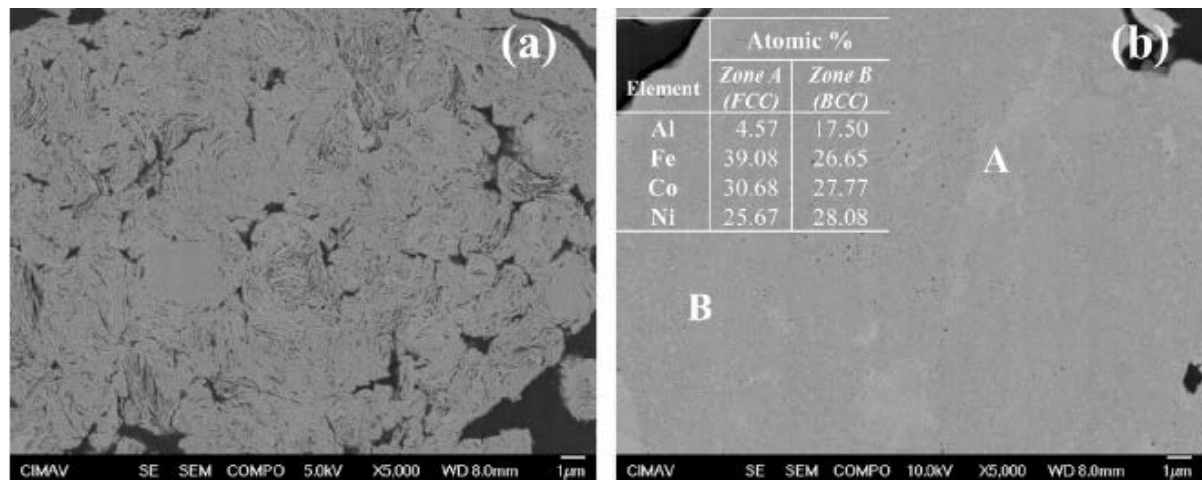


Fig. 4. Backscattered electron cross-section SEM micrographs of NiCoAlFe samples with 10 h of milling (a) alloyed powder and (b) annealed at 1473 K. The inset table shows the chemical composition of phases determined by an EDS-SEM analysis.

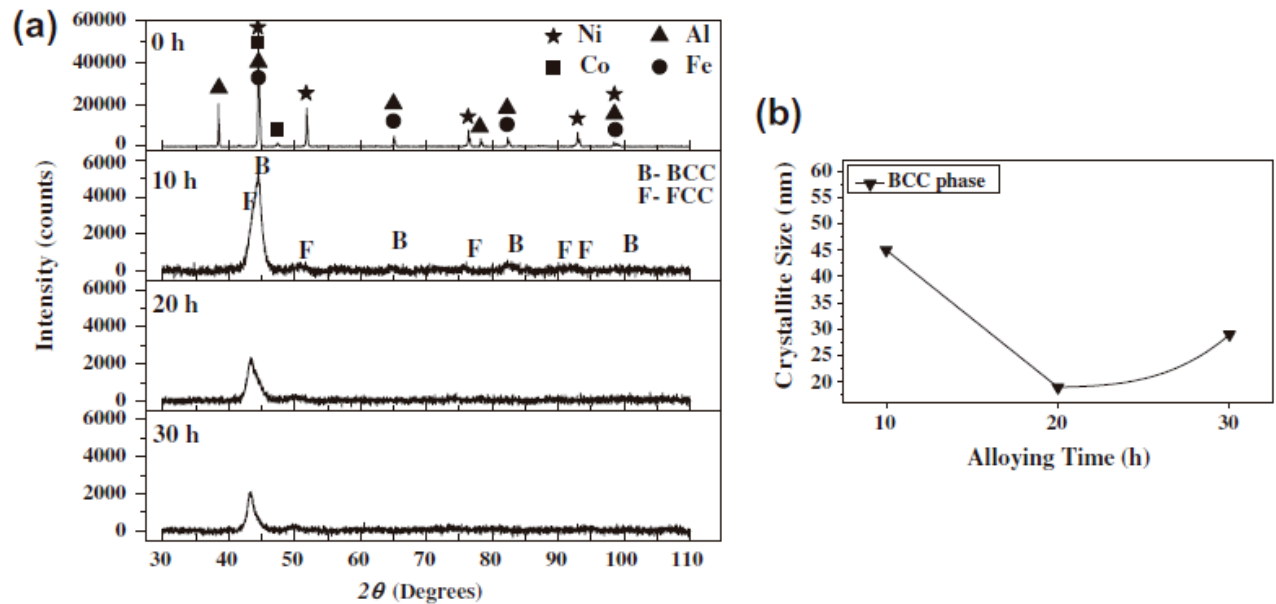


Fig. 5. (a) Structural evolution as a function of alloying time and (b) alloying time effect on crystallite size refining.

In the early stages of MA, the metal particles are still soft enough to be agglomerated. Usually a gradual refinement of particles is conducted; this is an indicative of the equilibrium state of the mechanical alloying process. The equilibrium between fracture and cold welding is achieved at different times for each system. In

ductile systems, an increase and homogenization of particle size is observed with the alloying time instead of the particle refinement. Fig. 2 shows the particle size distribution curves of MA'ed powders for each used alloying time. In the case of the sample with 10 h of MA, the particle size distribution is almost unimodal, non-symmetric with high particle sizes; a mean particle size ($d_{0.5}$) of 11.06 μm was measured. The curves of the samples with 20 and 30 h exhibit a bimodal distribution. Samples exhibit a mean particle size ($d_{0.5}$) of 38.67 and 49.42 μm , respectively. The results of mean particle size are supported by the surface area values of 0.41, 0.12 and 0.04 m^2/g , for the powders alloyed for 10, 20 and 30 h, respectively.

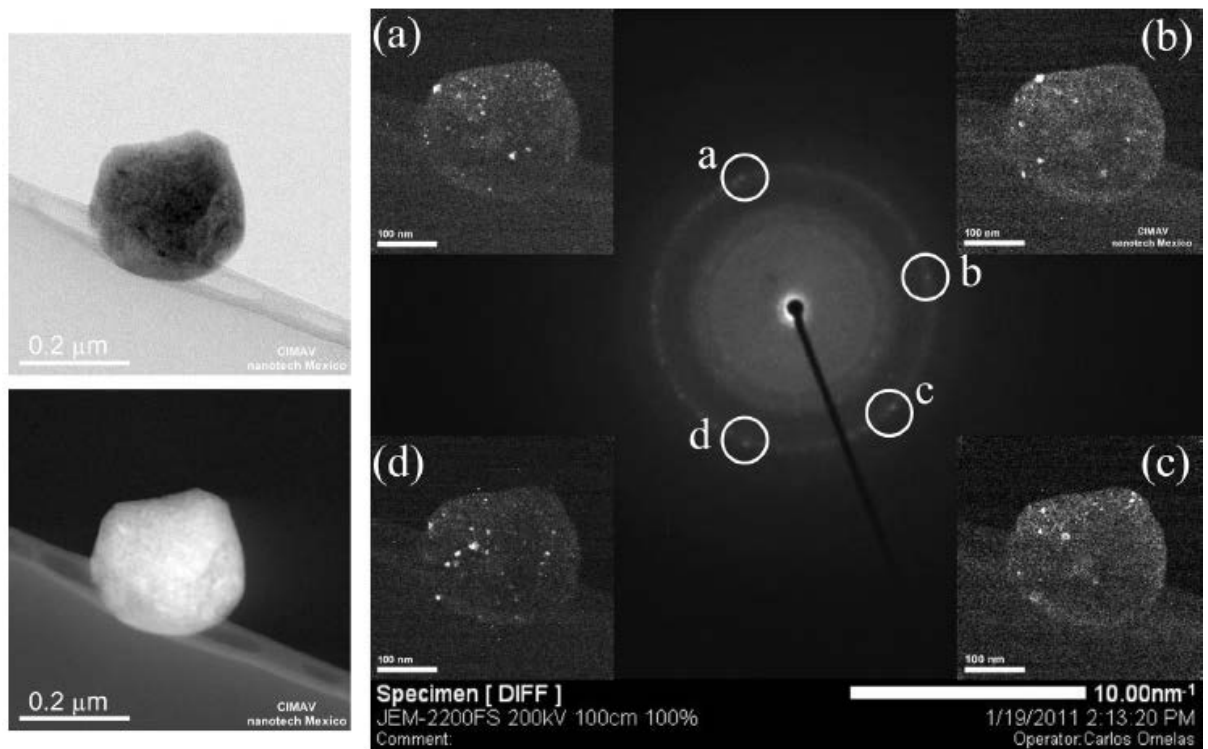


Fig. 6. TEM micrographs of NiCoAlFe sample after 30 h of alloying: (left) bright field and Z-contrast images in STEM mode, and (right) dark field images showing the nanoscale crystallite size.

All the particles will not have the same size in a common process of powder metallurgy. Several kinds of distribution size curves are expected during the measurement of MA'ed powders due to the shape of the nonspherical-formed particles. The different distribution curves can be interpreted according to the particle shape and their sizing method [6].

A reduction of the particle size is expected with further alloying time due to the work-hardening of particles. Contrary to expectations, the particle size is increased with the alloying time. However, the behavior of each system is different because there are several factors which could affect the milling process; some of them are powders ductility, the type of mill, the sample/milling media ratio and the amount of added PCA.

It has been reported that Fe–Ni–Co–Al (NCA) alloys with addition of other elements like Ta and B generates a state of super plasticity decreasing the precipitation of brittle phases in the grain boundaries [7]. Equiatomic composition promotes the increment of entropy and favors the formation of solid solution phases (FCC and/or BCC) instead of the formation of brittle intermetallic compounds [8–10] with results on improved ductility of the alloys.

For heat-treated powders, measurements of the mean particle size distribution were not appropriate because incipient sintering was shown on the particles (Fig. 3).

During MA, the particles formed by the cold welding of smaller particles have a typical lamellar microstructure (Fig. 4a). After the annealing process, it was observed that the internal pores of the particles were reduced and the lamellar

microstructure tended to disappear, leading to the formation of two distinguishable phases (Fig. 4b): a dark area having a chemical composition close to the equiatomic ratio, and a bright area having a low aluminum content.

Structural evolution and microstructural characteristics were monitored by XRD as a function of milling time (Fig. 5). Fig. 5a shows the evolution of powders mixtures with different alloying times. The XRD pattern identified as 0 h corresponds to the as-mixed powder sample. In this diffractogram, the characteristic reflections corresponding to pure elements Ni-FCC, Co-HCP, Al-FCC and Fe-BCC are observed. Milling time has noticeable effect on signal morphology [3]; for example, the peak intensity rapidly decreases with alloying time and with a longer time low intensity peaks disappear. The peaks of samples alloyed from 10 h became broad, which can suggest a microstructure refining from micro-crystalline ($\approx 2 \mu\text{m}$) to nanoscale ($< 50 \text{ nm}$). A noticeable peak shift is observed, suggesting the formation of solid solutions, with FCC and BCC structures.

Although there are different levels of solubility among the different elements, the formed solid solution phases after the mechanical alloying are composed of the four alloying elements. Aluminum with the alloying elements, in compositions near to the equiatomic ratios, Al (Co,Fe,Ni), exhibit the formation of a BCC solid solution (B2) [11] Al-Co, Al-Fe and Al-Ni, in compositions. The presence of this BCC solid solution phase can be explained by this solubility of Al with Co, Fe and Ni, even if the different used elements have different crystal structure.

With longer milling times, the secondary peaks of solid solutions are low in intensity, being hard to differentiate them from background. The main peak became

broader as the milling time increased from 10 to 20 h. It is well known that the grain refining and lattice distortion produce this peak broadening [3]. From the microstructural point of view, there are two causes for this phenomenon: an increment of grain boundary fraction and mechanical deformation. Between 20 and 30 h of alloying, the intensity of the main peak slightly decreases, but the broadening effect is not seen. This effect is reflected in the variation trend of the crystallite size as a function of alloying time (Fig. 5b).

The diffraction peaks broadening of the alloyed powders may indicate a crystallite size refining (nanoscale grains). Measurements of the full-width at half-maximum intensity (FWHM) were done to determine the crystallite size using the Scherrer's formula; only the BCC solid solution peaks could be measured. Crystallite size refining at 20 h can be observed, but with 30 h the crystallite size slightly increases. It was possible to corroborate that mechanically alloyed powders, through TEM observations of individual micro scale particles (Fig. 6) even after longer alloying times (30 h), are formed by nanocrystals without reaching a full state of amorphization. The rings present in the selected area diffraction pattern reveals a nanocrystalline microstructure.

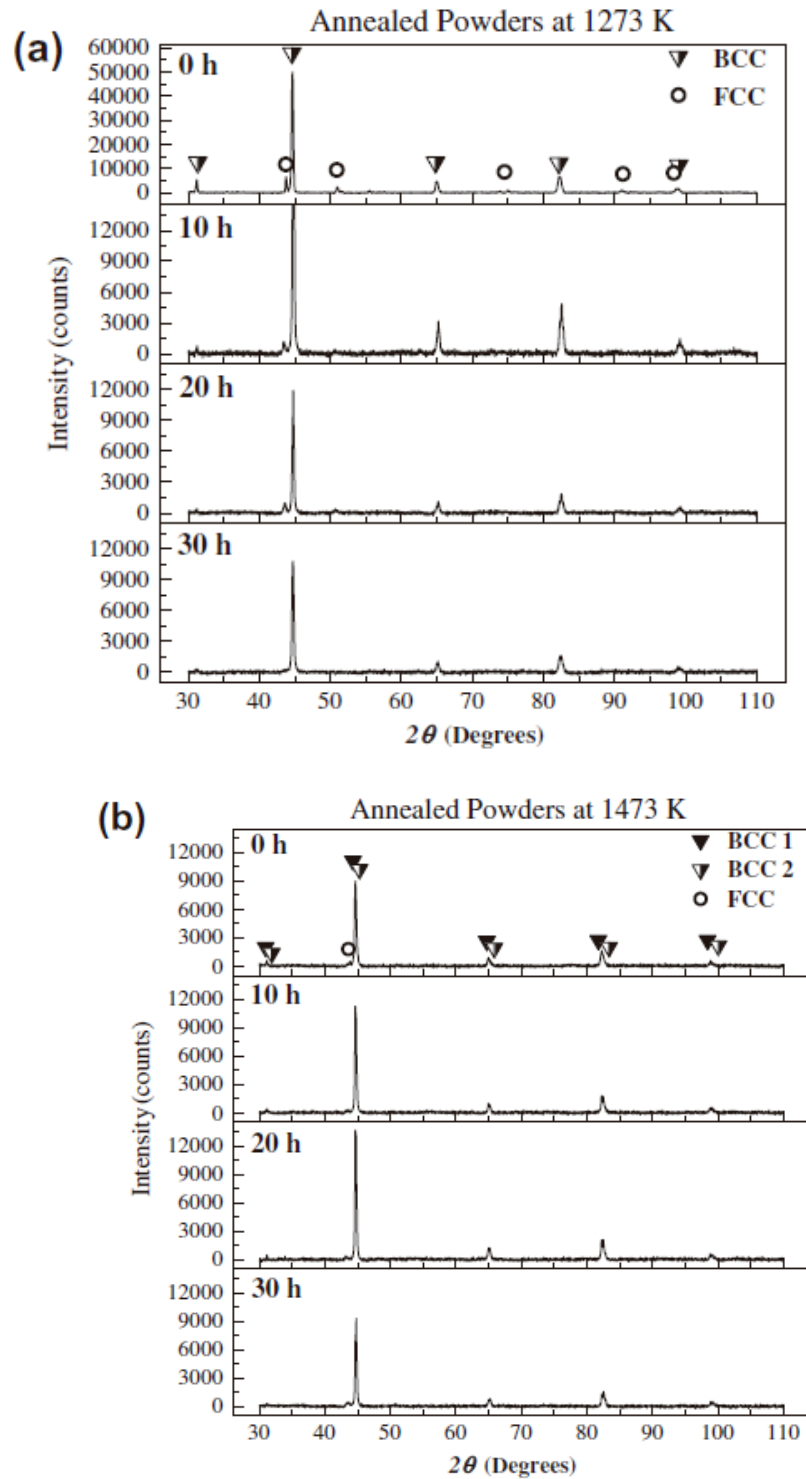


Fig. 7. XRD patterns of annealed powders at (a) 1273 K and (b) 1473 K as a function of alloying time.

The crystal size observed by TEM is much smaller (<10 nm) compared with calculated from the X-ray diffraction patterns.

Mechanical alloying introduces crystalline and microstructural defects (lattice strain and defect concentration); these phenomena in turn increase the enthalpy in alloys. The stored energy during mechanical alloying promotes the possible phase transformations and crystal growth during heat treatment [12]. Even though, crystal size in MA'ed and annealed products remains in the nanosize range.

For all XRD diffract grams of the annealed alloy powders (Fig. 7), peaks corresponding to a mixture of two phases (FCC + BCC) were observed. It is observed a domain in BCC phase over FCC phase on Fig. 7. The higher peaks that were observed correspond to BCC phase. The highest peak for BCC materials is generally generated by a (11 0) reflection, which is also easily observed in the annealed samples. The sharp and high intensity peaks reveal a higher degree of crystallinity in annealed powders. After annealing, the morphology in XRD patterns is very different compared to the one of the as-mechanically alloyed powders. This effect is not observed in unmilled powders. The increase of diffraction peaks intensity results from the micro strains release and crystallite size growth during the annealing process. However, the measurements of the FWHM using the Scherrer's formula indicate that even after annealing treatments, the crystallite size of MA'ed powders re-mains in nanoscale, between 40 and 56 nm for the BCC phase.

Regarding the heat treatment effect on milling products, Fig. 7a shows the XRD patterns of the powder annealed at 1273 K. After annealing treatment of mixed sample (0 h of milling) elemental peaks are not observed while the formation of two

solid solution phases is evident. A similar evolution is observed in milled and heat-treated samples. A Fe-like BCC phase and a FCC phase are identified. The BCC phases have a lattice parameter similar to pure Fe (0.286 nm). For the mixture (0 h), this parameter is 0.287 nm whereas it is 0.286 nm for all the as-mechanically alloyed powders. The lattice parameter of the FCC solid solution varies with the alloying time: 0.358, 0.361 and 0.360 nm, for 0, 10 and 20 h, respectively. The characteristic peaks from the FCC phase are no longer visible in the sample alloyed at 30 h.

The diffraction patterns of the powders annealed at 1473 K are shown in Fig. 7b. It can be seen the presence of peaks corresponding to two phases, one of them is an apparent ordered BCC structure and the second one is identified only for one peak and it corresponds to a FCC-like phase. The two BCC phases have similar lattice parameters, 0.286 and 0.287 nm (Table 2), which are unaffected by the alloying time. However, there is no evidence that they remain as ordered phases with 30 h of alloying. It has been re-ported that systems such as Fe–Co exhibit BCC structures [13], and CoAl, CoFe and CoNi systems present ordered structures (B2 type)[14]. It has been reported that, both, disorder and grain refinement are produced by the action of high-energy milling [15]. After heat treatments BCC phases appear but like ordered structures. On the other hand, the lattice parameter of the FCC phase exhibits a continuous change with the alloying time; it increased from 0 to 20 h and then decreased at 30 h. The lattice parameters are 0.357, 0.361, 0.363 and 0.361 nm for 0, 10, 20 and 30 h, respectively. The values of experimental lattice parameters are shown in Table 2.

Concerning the magnetic properties, Fig. 8 presents the plots of the

hysteresis loops as a function of alloying time and annealing temperature. The properties are summarized in Table 3.

In the as-mechanically alloyed samples the coercivity H_c reaches its highest value at 10 h (Fig. 9). Then, it slowly decreases and tends to stabilize with high alloying times (about 30 h). The initial increment in coercivity is due to refinement of crystallite size and defects introduced during the MA process, while the subsequent decrease is related to the phenomenon of random magnetic anisotropy.

Table 2
Lattice parameter (nm) of the annealed powders.

	Alloying time											
	0 h			10 h			20 h			30 h		
	FCC	BCC1	BCC2	FCC	BCC 1	BCC 2	FCC	BCC 1	BCC 2	FCC	BCC 1	BCC 2
1273 K	0.358	0.287	-	0.361	0.286	-	0.360	0.286	-	-	0.286	-
1473 K	0.357	0.286	0.286	0.361	0.287	0.286	0.363	0.287	0.286	0.361	0.287	0.286

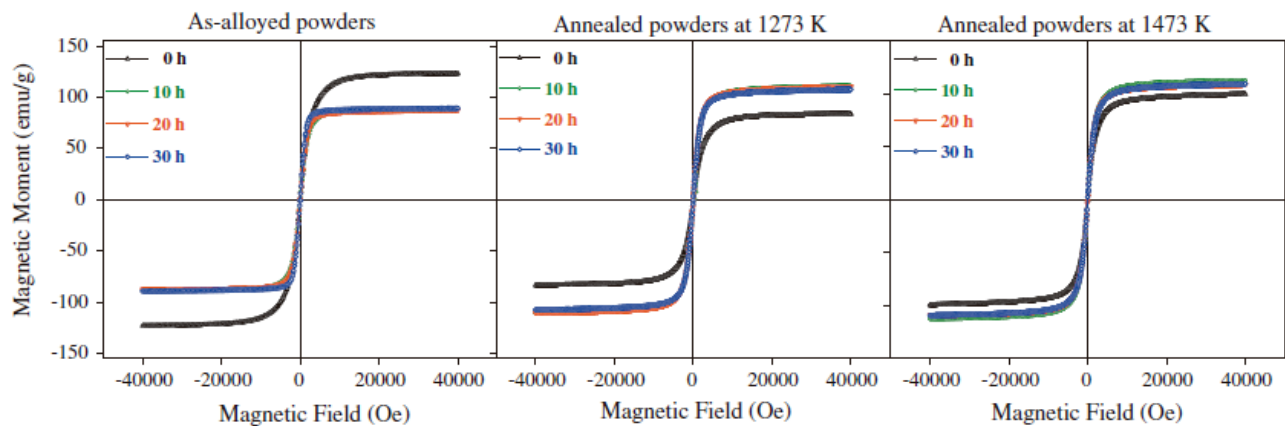


Fig. 8. Hysteresis loop variation of the NiCoAlFe system with alloying time and annealing temperature.

Table 3
Magnetic properties of NiCoAlFe powder alloys.

System	Alloying Time (h)	σ_{max} (emu/g) at $H_{max} = 40,000$ Oe	σ_r (emu/g)	Coercivity H_c (Oe)
MA'ed powders	0	123.27	1.40	35.10
	10	88.99	6.06	167.51
	20	88.22	2.96	72.17
	30	89.50	1.04	21.76
Annealed powders at 1273 K	0	83.57	0.36	5.75
	10	111.25	5.57	117.78
	20	110.47	5.18	106.62
	30	107.58	4.12	91.42
Annealed powders at 1473 K	0	99.53	0.69	12.92
	10	112.73	3.23	60.63
	20	108.99	3.56	80.97
	30	109.34	4.69	94.83

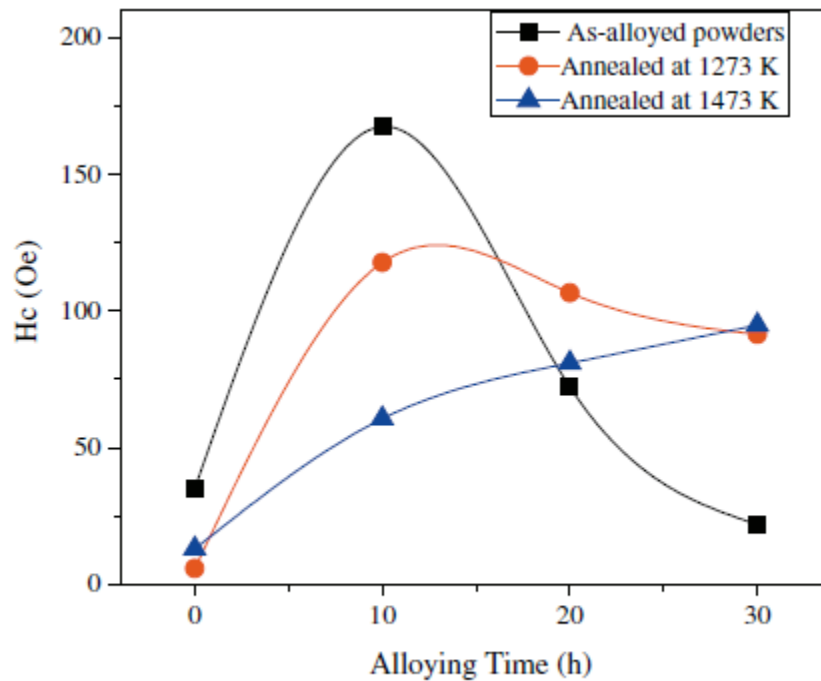


Fig. 9. Coercivity of NiCoAlFe powders as a function of alloying time.

A similar behavior is observed in a slighter way in samples annealed at 1273 K, which is due to the increasing of crystallite size and decreasing of defects. However, the behavior of the coercivity as a function of alloying time is different for the samples annealed at 1473 K, where a steady increase of the coercivity is observed. In this case, the crystallite size increased enough (even with longer alloying times), avoiding the phenomenon of random magnetic anisotropy.

Remanent magnetization r_r curves as a function of alloying time (Fig. 10) show a similar behavior to the coercivity curves. Such behavior is related to a roughly proportional dependence of the coercivity with the remanent magnetization.

The atoms on the surface of the nanocrystals form a significant portion of their whole volume. These atoms generate a high surface magnetic anisotropy due to the increase of grain surface area and the greater interaction with the nearest neighbor atoms. This effect makes hard to complete saturation of magnetization even with an applied magnetic field of 40 kOe. For the as-alloyed powders, the dependence of the maximum magnetization r_{max} for a maximum applied magnetic field of 40 kOe, as a function of the alloying time, shows an abrupt initial decrease of magnetization at 10 h, and a slight increase for greater alloying time (30 h). Annealed samples at both 1273 and 1473 K temperatures show an opposite behavior in comparison with the MA'ed samples. The magnetization increases when reaching 10 h of milling, while at 20 and 30 h they exhibit a slight decrease of magnetization. The complex evolution of magnetic properties has a direct relationship with the different contribution of the phases formed during the heat treatments.

4. Conclusions

A NiCoAlFe powder alloy was successfully synthesized through high-energy milling from equiatomic elemental powder mixtures. The following conclusions are listed:

- (1) The presence of simple BCC and FCC phases in both as-mechanically alloyed and annealed powders was observed.
- (2) Nanometric crystallite size was observed in the alloyed powders while slightly grain growth, after annealing, was observed.
- (3) Temperature has a significant effect on the formation of phases and crystallite size. Two phases, FCC and BCC, are formed at 1273 K while a second BCC phase appears at 1473 K.
- (4) The lattice parameter of BCC phases remains nearly constant for all the alloying times and both temperatures ($a_{\text{BCC}} \approx 0.286 \text{ nm}$). The lattice parameter of FCC phases slightly increased with the alloying time but the changes are not significant in consideration to the temperature of the annealed treatment.
- (5) In the as-alloyed powders and the annealed samples at 1273 K, the coercivity increases with the alloying time due to the grain size and random magnetic anisotropy. This phenomenon was slightly lower in the heat-treated samples at

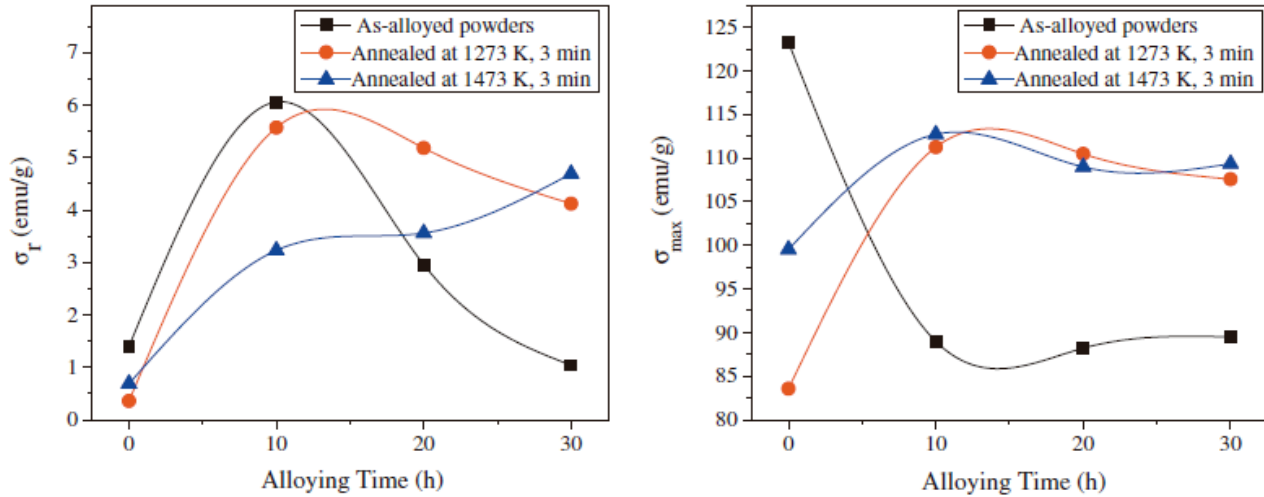


Fig. 10. Magnetization curves of the NiCoAlFe systems at different alloying times.

1473 K due to crystals growth caused by the increase in temperature.

Magnetic properties are strongly affected by the phases formed after annealing.

Acknowledgments

This research was supported by CONACYT-Red Temática de Nanociencias y Nanotecnología and Red Temática de Ciencia y Tecnología Espaciales (0124623, 0124891, 0170224 and 0170617). The authors would like to thank the technical assistance of K. Campos-Venegas, W. Antúnez-Flores, E. Torres-Moye and J.E. Ledezma-Sillas.

References

- [1] J.W. Yeh, Y.L. Chen, S.J. Lin, S.K. Chen, Mater. Sci. Forum 560 (2007) 1–9.
- [2] J.W. Yeh, S.K. Chen, S.J. Lin, J.Y. Gan, T.S. Chin, T.T. Shun, C.H. Tsau, S.Y. Chang, Adv. Eng. Mater. 6 (2004) 299–303.
- [3] C. Suryanarayana, Prog. Mater. Sci. 46 (2001) 1–184.

- [4] Y. Liu, J. Zhang, L. Yu, G. Jia, C. Jing, S. Cao, J. Alloys Comp. 377 (2004) 202–206.
- [5] T. Sourmail, Scripta Mater. 51 (2004) 589–591.
- [6] G.S. Upadhyaya, Powder Metallurgy Technology, Cambridge International Science Publishing, 1997.
- [7] T. Omori, S. Abe, Y. Tanaka, D.Y. Lee, K. Ishida, R. Kainuma, Thermoelastic martensitic transformation and superelasticity in Fe–Ni–Co–Al–Nb–B polycrystalline alloy, Scripta Mater. 69 (2013) 812–815.
- [8] B.S. Li, Y.P. Wang, M.X. Ren, C. Yang, H.Z. Fu, Mater. Sci. Eng. A 498 (2008) 482–486.
- [9] A. Li, X. Zhang, Acta Metall. Sin. 22 (2009) 219–224 (Engl. Lett.).
- [10] K.B. Zhang, Z.Y. Fu, J.Y. Zhang, W.M. Wang, H. Wang, Y.C. Wang, Q.J. Zhang, J. Shi, Mater. Sci. Eng. A 508 (2009) 214–219.
- [11] T.B. Massalski, H. Okamoto, P.R. Subramanian, L. Kacprzak, W.W. Scott, Binary Alloy Phase Diagrams, American Society for Metals, 2001.
- [12] M. Sluiter, Y. Kawazoe, Acta Mater. 47 (1999) 475–480.
- [13] S. Bergheul, H. Tafat, M. Azzaz, J. Mater. Eng. Perform 15 (2006) 349–351.
- [14] H.J. Al-Kanani, J.G. Booth, J. Magn. Mater. 139 (1995) 299–311.
- [15] S. Gialanella, X. Amils, M.D. Barò, P. Delcroix, G. Le Caër, L. Lutterotti, S. Suriñach, Acta Mater. 46 (1998) 3305–3316.